

**N 68-27385**

(ACCESSION NUMBER)

(THRU)

(PAGES)

(CODE)

(NASA CR OR TMX OR AD NUMBER)

(CATEGORY)



GPO PRICE \$ \_\_\_\_\_

CFSTI PRICE(S) \$ \_\_\_\_\_

Hard copy (HC) \_\_\_\_\_

Microfilm (MF) \_\_\_\_\_

#653 July 65

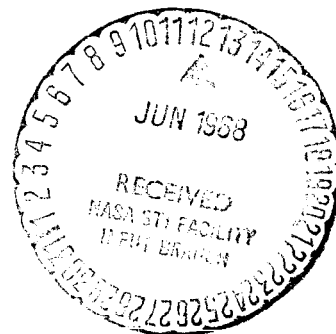
DEPARTMENT OF

**SPACE SCIENCE**



RICE UNIVERSITY

HOUSTON, TEXAS



FACILITY FORM 7

On the Variety of Particle Phenomena  
Discernible at the Geostationary Orbit  
via the ATS-1 Satellite\*

by

J. W. Freeman, Jr. and J. J. Maguire\*\*

Department of Space Science  
Rice University  
Houston, Texas 77001 U. S. A.

Paper presented at the Birkeland Symposium  
on Aurora and Magnetic Storms, Sandefjord,  
Norway, September, 1967, and submitted to the  
Annales de Géophysique.

\*Research supported by NASA Contract NAS5-9561. ✓

\*\*Present address: Department of Physics, Boston College,  
Chestnut Hill, Massachusetts, U. S. A.

## ABSTRACT

The purpose of this paper is to provide a brief catalog of the three most salient phenomena that have been observed with the Rice University ion detector aboard the ATS-1 synchronous orbit satellite. These phenomena are, a gross pre-post/midnight asymmetry in the enhanced energetic charged particle fluxes observed on the night side of the earth, a magnetopause penetration to  $6.5 R_E$  with the subsequent detection of discreet clouds of energetic particles executing repeated longitudinal drift about the earth, and bursts of very low energy,  $E < 50$  eV, highly directional positive ions tentatively associated with hydromagnetic transients. Each of these phenomena are described in sufficient detail to illustrate the prominent facts.

## I. Introduction

It has been recognized for some time that the geostationary (or synchronous) orbit offers interesting and unique advantages for the study of magnetospheric phenomena. For example, the fact that such a satellite sweeps through all local times in a 24 hour period at a nearly constant altitude makes possible the study of gross local time particle asymmetries near the equatorial plane field lines which intersect the earth in the auroral latitudes. In addition large scale magnetospheric convection patterns of the magnetospheric plasma can, at least in principle, be detected and plotted over time intervals short compared with magnetic storm periods. The longitudinal drift times and degree of temporal stability of discrete clouds of energetic particles can be determined as the clouds are encountered by the satellite on successive orbits about the earth, and so on.

In December of last year the United States successfully launched the first of its Application Technology Satellites, ATS-1 (shown in the first figure). The satellite is in a synchronous orbit that is circular at  $6.5 R_E$  geocentric distance. It has a nearly  $0^\circ$  inclination and is "parked" at  $150^\circ$  West longitude.

The satellite is primarily a communications and engineering satellite, however approximately 40 lbs. of the 600 lbs. payload were allocated for scientific experiments.

The Rice University ion detector aboard this geostationary satellite was primarily intended to search for convective

and hydromagnetic wave induced motions in the magnetospheric thermal plasma, consequently it was designed with positive ion energy resolution in the 0 to 50 eV range via 20 differential energy pass-bands. The instrument consists of a funnel channel electron multiplier coupled with a planar retarding potential analyzer. The 20 energy pass-bands result from square-wave modulation of a retarding potential grid. In addition, two integral energy channels, one at 0 eV and one at 50 eV, are included in the instrument sequencing program. In the integral energy channel mode the voltage on the retarding potential grid is held fixed at either 0 or 50 volts, and counts from the channel electron-multiplier are fed directly to an adaptive accumulator. The input aperture of the channel electron-multiplier is biased continuously at -3000 volts so that the instrument is insensitive to electrons below 3 keV, but in the 0 integral energy channel it maintains a nearly uniform efficiency to positive ions from thermal energies to several hundred keV and electrons above 3 keV. The instrument directional geometric factor is  $10^{-3} \text{ cm}^2\text{-ster}$ . including detection efficiency.

The satellite spins at approximately 97 RPM, and as it does so the counts from the channel electron multiplier are segmented in time, so that the directions of arrival of the incoming particles are divided into thirty discrete sectors, each  $12^\circ$  apart and including an angular field of view of about  $25^\circ$ . The detector look directions are normal to the spin axis of the satellite, which in turn is parallel to the spin

axis of the earth. Thus the detector scans look directions roughly in the magnetic equatorial plane of the earth.

The time limit on this paper precludes a complete discussion of all of the phenomena observed to date with the Rice ATS-1 ion detector. I will attempt instead to provide a thumbnail sketch of each of three different phenomena in an effort to present the kinds of things that have been observed.

II. Phenomena #1: The Gross Local Time Asymmetry of the Energetic Particle Population near the Midnight Meridian [Freeman and Maguire, 1967].

The next figure (Figure 2) illustrates a typical counting-rate profile for the ion detector on one complete orbit during a period of moderate magnetic disturbance ( $\Sigma K_p$  10 to 17). The ordinate is the approximate counts per accumulation interval and the abscissa, universal time. The data plotted represent all positive ions above 0 energy or more correctly, the satellite potential and all electrons above approximately 3 keV. In this mode of operation the instrument can be thought of as a total particle detector except for electrons below 3 keV. (Note that for equal proton and electron volume number densities and identical energy spectra the electrons will be the more commonly observed particles because their lower masses require higher velocities for the same energy). No detectable fraction of the flux consists of positive ions in the 0 to 50 eV energy range. The data plotted are from the fluxes whose direction of arrival is the anti-solar direction, however, this is not important for our purpose since these fluxes are isotropic

in the equatorial plane, at least to first order. The striking feature of the data is the sharp rise in the particle flux as the satellite crosses the midnight meridian heading toward the midnight-to-dawn quadrant. This graph is typical of a moderate magnetically disturbed period. A quiet period would show no rise near midnight but would remain about at the pre-midnight level throughout the entire 24 hour period.

As the intensity of magnetic disturbance increases the local time of the rise decreases, that is, the rise moves to the left on this graph. The next figure (Figure 3) shows the equivalent graphs for four successive days of a more highly disturbed period. The  $\Sigma K_p$  sums for these four days are 19, 23, 30 and 35 respectively. On these four consecutive days one can see that there has been a general broadening of the region of local times over which the enhanced particle fluxes occur. Note that there does appear to be some residual of the pre/post-midnight asymmetry effect observed in the moderately disturbed cases, and that for the final two days in the sequence one can still see some remnants of the sharp rise time. The intensity of the particle flux does not appear to be correlated with the  $K_p$  index, but rather the general breadth of the disturbance in local time seems to be the correlating factor.

Figure 4 shows the College, Alaska magnetogram horizontal component for the same four days. Without looking at a detailed comparison it can be seen that the magnetic disturbances at College show the same general time distribution as the

particle fluxes on the ATS satellite. We can see, for example, this tendency for the region of distribution to broaden out in local time as the storm grows in intensity. Also, we can see generally some relationship between the maximum regions of magnetic disturbance and the maximum particle flux enhancements. A study is currently underway on the relationships between the detailed variations in the ATS particle fluxes and the ground observations including all-sky camera films.

Figure 5 is a pictorial diagram of the pattern which is being evidenced here. Here we have an equatorial cross section of the magnetosphere, and in Part a of this figure is represented the magnetic quiet time conditions. Here there may exist some region of enhanced plasma or disturbance, but it lies sufficiently far out in the tail that the synchronous orbit does not intersect it. In Figure 5b the magnetic activity has increased to the point where the inner edge of this region of enhancement has been driven inward to intercept the satellite trajectory. The leading edge, or in particular the pre-midnight edge of this region of enhancement, is shown to be very sharp. Also in evidence here is the pre-post/midnight asymmetry. In Figure 5c we have the condition present during the most intense magnetic disturbances, when the enhanced particle region has apparently moved inward from the tail. Now the region of enhancement extends in some cases as far around as the dawn meridian. We believe that the gross picture provided by the data is consistent with the large scale inward motion of a large region of enhancement,



and that the general particle fluxes in this region appear to wax and wane in concert with the polar substorm activity, as indicated by the magnetograms at high latitude.

### III. Phenomena #2: Observation of the Magnetospheric Boundary and Subsequent Particle Clouds

Until now, all the data presented have related to phenomena in which the particle fluxes were isotropic (at least to first order), and for which there was no important fraction of the total proton flux in the 0 to 50 electron volt energy range. We shall now present data for which neither of these two situations is true.

On January 13, 1967 a substantial magnetic storm commenced. Figure 6 shows the Honolulu, San Juan and Guam magnetograms for this event. At noon U.T. on the 13th there occurred two remarkable square-wave sudden impulses, but from then on the storm appears to develop rather gradually, with the initial phase lasting until about 2100 or 2200 hours on the 13th. About three hours into the main phase, shortly after the first hour on the 14th, there occurred a positive spike. At the time of this sudden impulse, the ATS satellite was about 2 and 1/2 hours past the noon meridian and heading toward the dusk meridian. The January 14 data from one of the angular distribution samples, or one of the rotations of the satellite, is shown in Figure 7.

This group of graphs shows the fluxes from five different directions all plotted on the same abscissa. Note the top

graph, which corresponds to the fluxes coming from a range of about  $36^{\circ}$  to  $60^{\circ}$  clockwise from the satellite-sun direction. There is a very pronounced peak in the particle flux during the first hour. There follows a second peak at around 4:00, then another at 6:30, and (although it isn't clear from this figure because noisy data has been automatically removed by the computer plot program) yet a third peak at about 9:00. As we move down the ordinate of Figure 7, i.e., in directions away from the sun, the initial peak diminishes in intensity until we get to the bottom curve (which corresponds to fluxes coming from the antisolar direction). There the first peak has disappeared altogether. However, we see that the subsequent peaks are still present. Thus, during the period of one-half hour or so in the first part of the day, there was an intensely anisotropic flux. That anisotropic flux was then followed by successive peaks which were almost completely isotropic and separated in time by about 2 and 1/2 hour intervals.

The degree of anisotropy of the particle flux in the first peak can be seen in Figure 8, where particle flux is plotted as a function of the direction of arrival. One can see that there is a maximum number of counts per accumulation interval which occurred at around  $45^{\circ}$ . The plot is made on a linear scale, so that one can readily see that the front to back ratio for this anisotropy is almost an order of magnitude. Figure 9 shows a diagrammatic representation of what was observed on January 14. Here we've plotted along the satellite trajectory the observation points of these four particle bursts. Vectors have been drawn to indicate the magnitude and direction

of the particle fluxes. In the first burst at about 2 and 1/2 hours after noon one can easily discern very intense anisotropic fluxes, with the direction of arrival roughly tangent to the satellite orbit. The following three successive bursts appear to be relatively isotropic, but of gradually diminishing overall amplitude. Based on the data from the two integral channels of the ion detector the flux observed during the anisotropic burst contained a fraction of approximately 10% positive ions whose energy was below 50 eV.

We interpret the data from the anisotropic flux period to indicate that the magnetopause was temporarily compressed beyond  $6.5 R_E$ , so that the satellite temporarily entered the magnetosheath. The U.C.L.A. magnetometer [Cummings and Coleman, 1967] showed sudden changes in the local magnetic field magnitude and direction at the times of these large scale anisotropic fluxes. This is consistent with the idea of a boundary crossing as is the high directional flux and soft spectrum observed by the ion detector.

Further, we suggest that the three successive isotropic bursts subsequent to the anisotropic burst may represent encounters of the satellite with a single cloud of energetic particles drifting in longitude around the earth. Based on the observed time between bursts of two hours and twenty-five minutes and assuming an axisymmetric magnetic field, the energies required of such particles are 40 keV if the particles are protons and 50 keV if electrons. In an attempt to discern whether or not these successive peaks are observations of the

same cloud we have replotted the data in high time resolution. The result, shown in Figure 10, is an overlay of the fluxes of the three isotropic bursts. One can see that there apparently are individual peaks in the first burst that can also be found in the second. If this hypothesis is correct, the entire cloud must have been monoenergetic to within 1 keV, or a few percent, and the individual temporal variations merely mirror the time profile of the injection mechanism.

IV. Phenomena #3: Bursts of Very Low Energy, Highly Directional Positive Ions Within the Magnetosphere

At approximately 0145 U.T. on the 8th of January 1967 the ATS ion detector registered a remarkable highly directional flux of positive ions whose energies were below 50 eV. The angular distribution of this flux (integral flux above 0 eV) is shown for one angular scan in Figure 11. The direction of arrival of the flux is roughly the antisolar direction. The flux intensity was sufficiently great that an energy spectrum could be obtained through the ion detector differential energy channels. The measured differential spectrum shows a narrow energy peak centered on 5 eV, however, the exact value of the mean energy must remain uncertain because of the unknown satellite potential. Two additional similar events have been found in the ATS data examined to date. Under normal conditions the ion detector registers no statistically significant counts in the 0 to 50 eV energy range (i.e.,  $j \leq 5 \times 10^5$  particles  $\text{cm}^{-2} \text{sec}^{-1} \text{ster}^{-1}$ ).

These anisotropic fluxes may result from the directional

motion of the thermal plasma induced by the passage of a transient hydromagnetic wave or alternatively they may represent the continuous convection currents flowing throughout the magnetosphere but having been made visible to the ion detector by a temporary increase in the requisite D.C. electric fields. If the latter hypothesis is correct an electric field of the order of several millivolts per meter is required to produce the observed  $\vec{E} \times \vec{B}$  drift motion for protons assuming an insignificant spacecraft potential. If the former hypothesis is dominant hydromagnetic transients of amplitude approximately one third the ambient field are required for hm wave velocities of the order of 100 km/sec. It is hoped that a complete examination of the on-board and ground-based magnetometer data will help resolve the exact nature of this flux.

V. Acknowledgments

We appreciate helpful discussions with Prof. A. J. Dessler. This research was supported under NASA Contract NAS5-9561.

REFERENCES

Cummings, W. D., and P. J. Coleman, Jr., Simultaneous magnetic field variations at the earth's surface and at the synchronous, equatorial distance, Conjugate Point Symposium, June, 1967.

Freeman, J. W. and J. J. Maguire, Gross local time particle asymmetries at the synchronous orbit, to be published in the J. Geophys. Res., November, 1967.

CAPTIONS FOR FIGURES

- Figure 1            The ATS-1 Satellite
- Figure 2            Figure 2 shows the response of the ATS ion detector to particles flowing from the anti-solar direction during a moderate magnetically disturbed day. The ordinate, level number, is a non-linear representation of the counts in each accumulation interval. Level No. 8 corresponds to a flux of approximately  $3 \times 10^6$  ions/cm<sup>2</sup>-sec.-ster., Level No. 24 to  $1 \times 10^7$  ions/cm<sup>2</sup>-sec.-ster., and Level No. 40 to  $4 \times 10^7$  ions/cm<sup>2</sup>-sec.-ster.
- Figure 3            Figure 3 shows a composite set of ion detector data for four days during a magnetically disturbed period. The ordinate specifications for Figure 2 apply to these data also.
- Figure 4            A composite set of magnetograms from College, Alaska for the days 358 through 361, 1966.
- Figure 5            A diagrammatic representation of the motion of region of enhanced plasma fluxes in the equatorial plane during disturbed magnetic conditions. Part (a) shows the hypothetical plasma region outside the geostationary orbit during quiet magnetic periods. Part (b) shows the penetration of a portion of the plasma

to  $6.5 R_E$  with increasing magnetic disturbance; this plasma being concentrated near the midnight meridian. Part (c) shows the bulk of the plasma region moving into the body of the magnetosphere during intense magnetic activity.

Figure 6 Magnetograms showing the horizontal component of the geomagnetic field at San Juan, Honolulu, and Guam during the magnetic storm of January 13-14, 1967.

Figure 7. ATS particle flux data from the 0 eV integral channel for Day 14, 1967. This set of graphs gives the fluxes from five different look directions of the detector plotted on a common abscissa. The ordinate, level number, is a non-linear representation of the counts in each accumulation interval. The conversion to flux is approximately as follows: Level No. 8 corresponds to a flux of  $3 \times 10^6$  ions/cm<sup>2</sup>-sec.-ster., Level No. 24 to  $1 \times 10^7$  ions/cm<sup>2</sup>-sec.-ster., and Level No. 40 to  $4 \times 10^7$  ions/cm<sup>2</sup>-sec.-ster. Each ordinate scale marking corresponds to a multiple of 10 (level numbers) with a sliding zero assigned to each of the five curves.

Figure 8 Linear plot of particle flux vs. direction of arrival for the anisotropic flux event at the beginning of Day 14, 1967.



- Figure 9 Day 14 satellite trajectory, with anisotropic and isotropic bursts indicated. The arrows are vectors, giving both the magnitude and direction of flux at the particular local time.
- Figure 10 Triple overlay of the three isotropic bursts in high time resolution. The abscissa is so arranged that corresponding points on graphs A, B, and C are separated in time by 2 hours and 25 minutes. The maximum amplitude on curve A corresponds to approximately 1000 counts, and the three curves must be connected in order end to end in order to read the ordinate. Again, the ordinate is a non-linear scale, but here each point represents a channel sum for intervals as small as 1 minute and 53 seconds.
- Figure 11 Angular distribution of the very low energy protons.

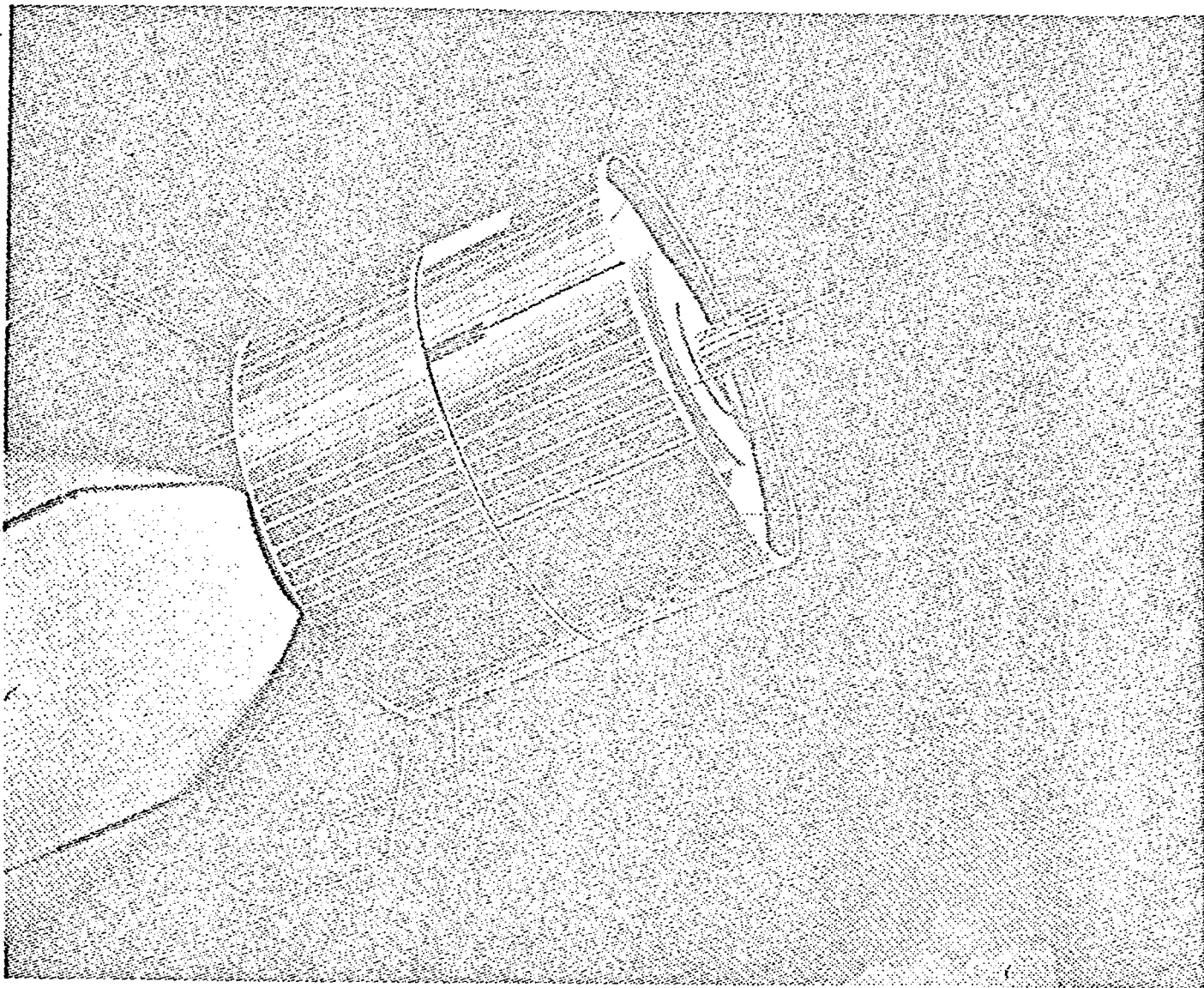


Figure II-1. Spin Stabilized  
Synchronous Altitude Spacecraft

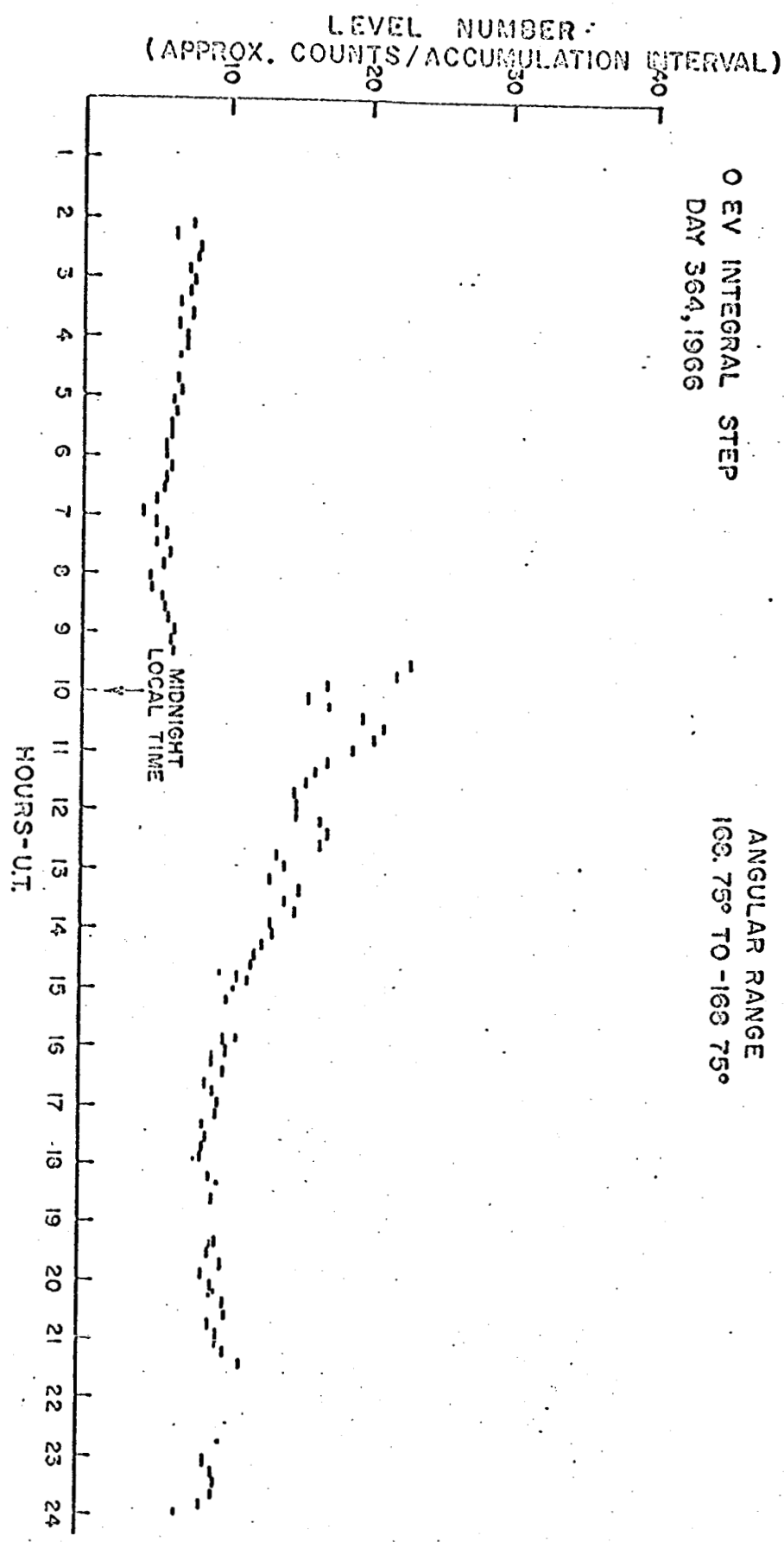


FIGURE 2

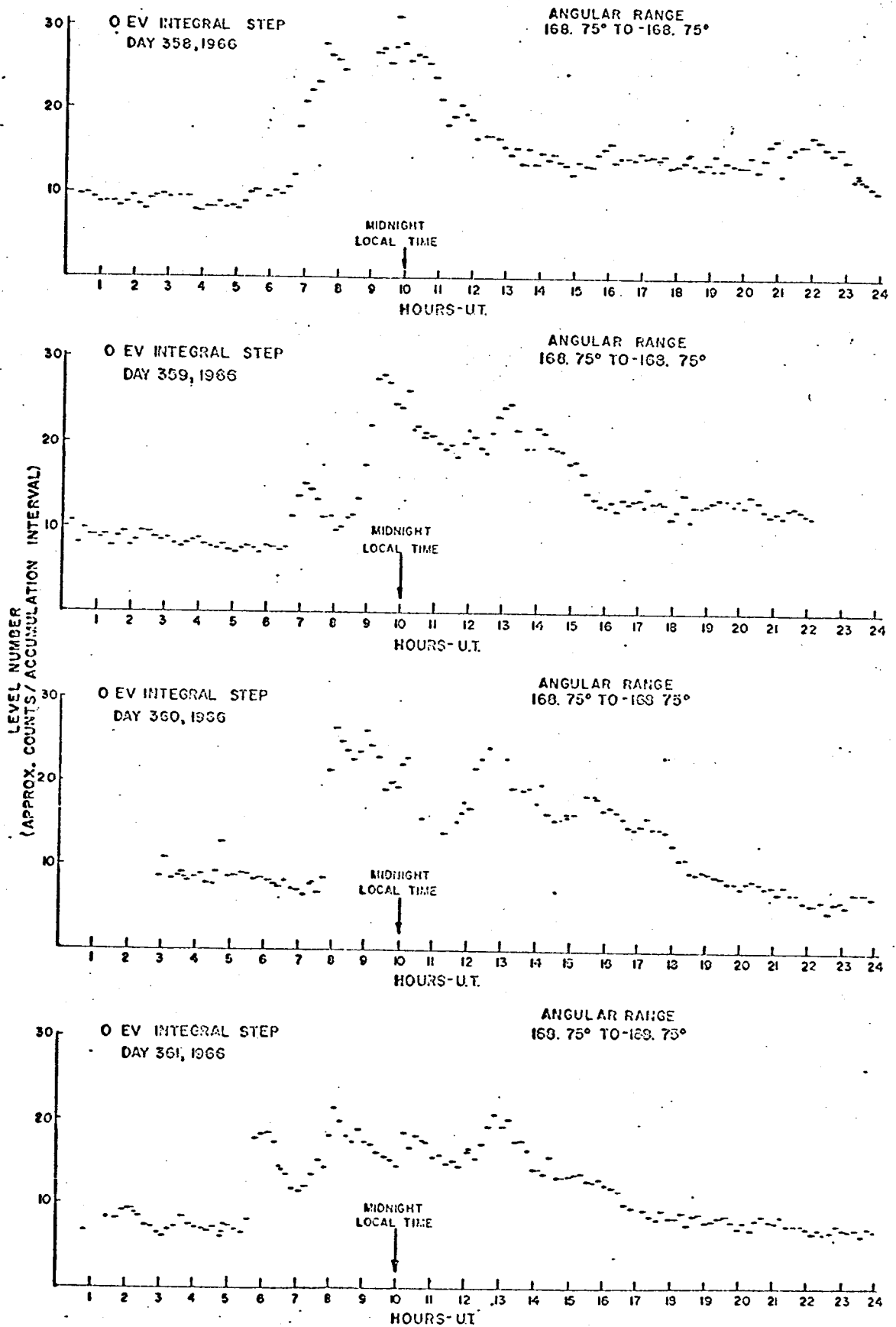


FIGURE 3

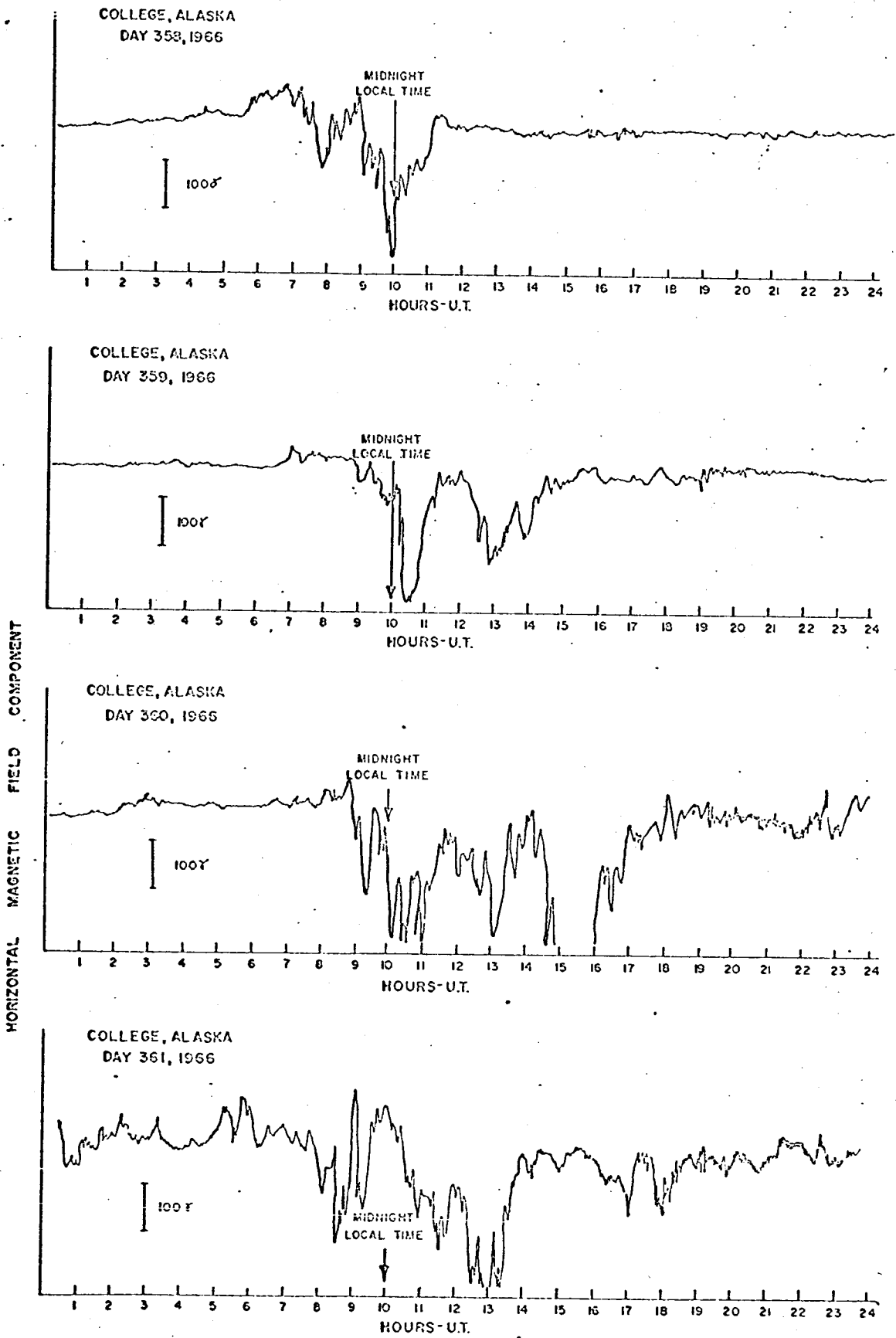


FIGURE 4

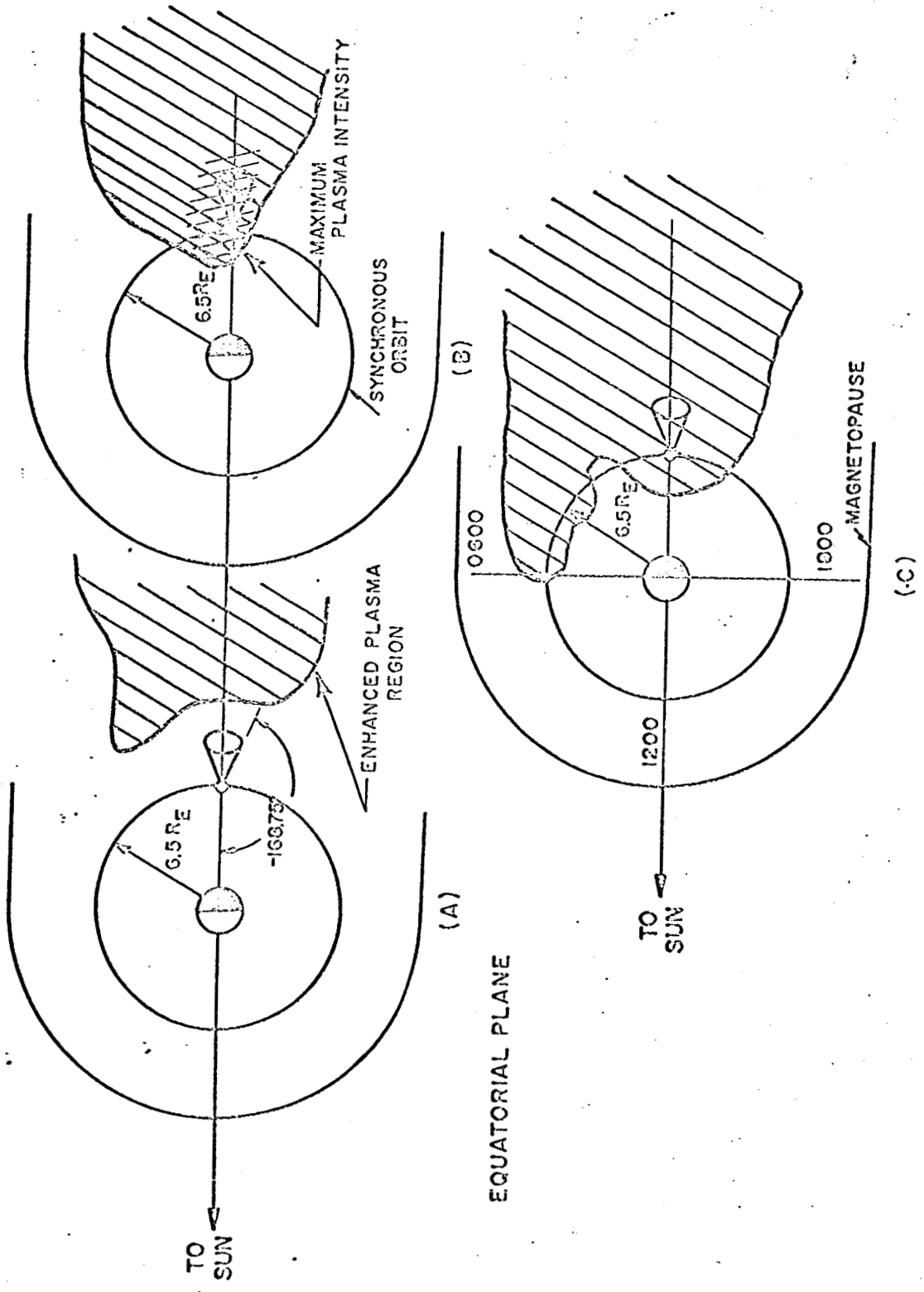
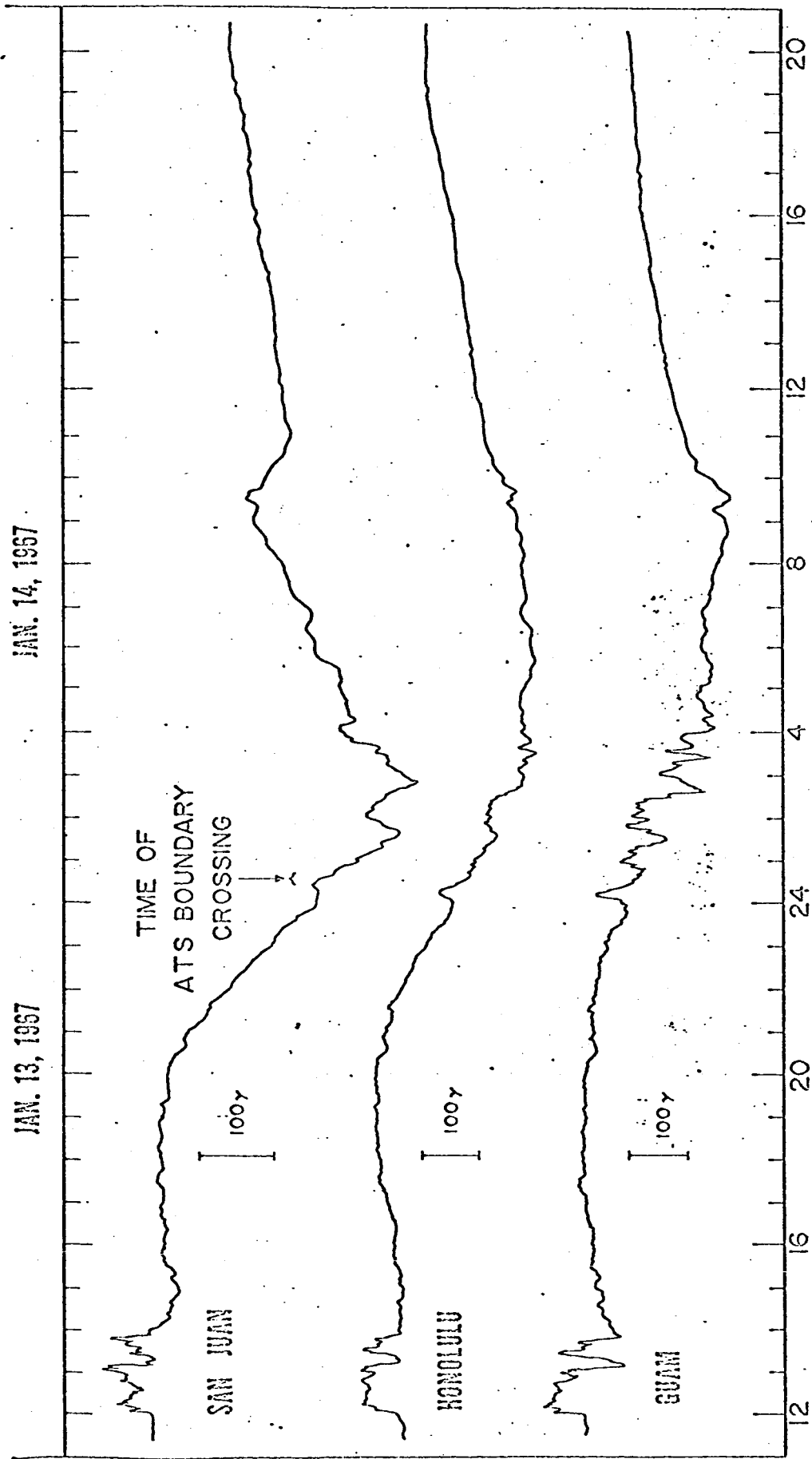


FIGURE 5



U.T.

Figure 6

LEVEL NUMBER  
(APPROX. COUNTS/ACCUMULATION INTERVAL)

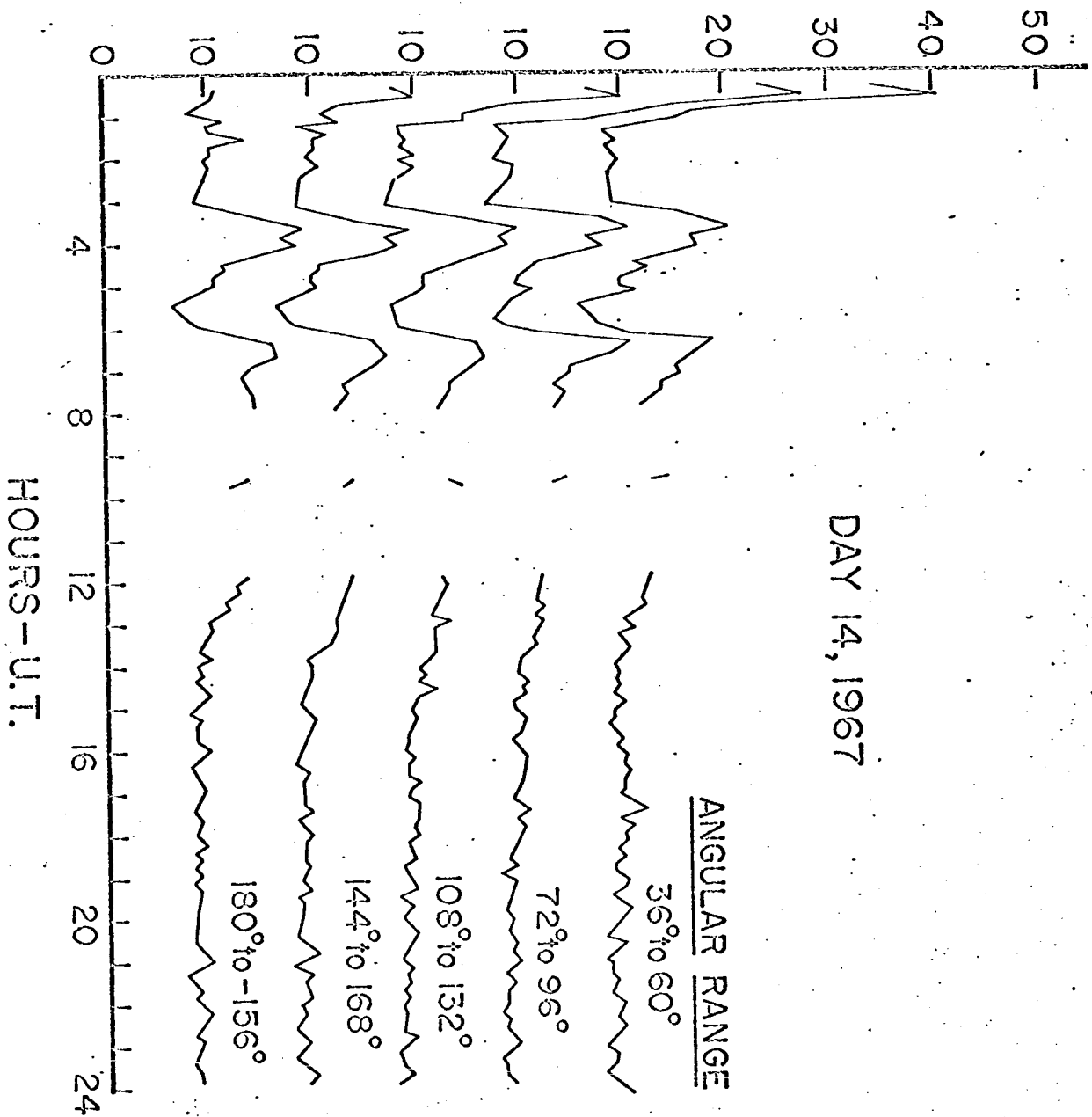


Figure 7



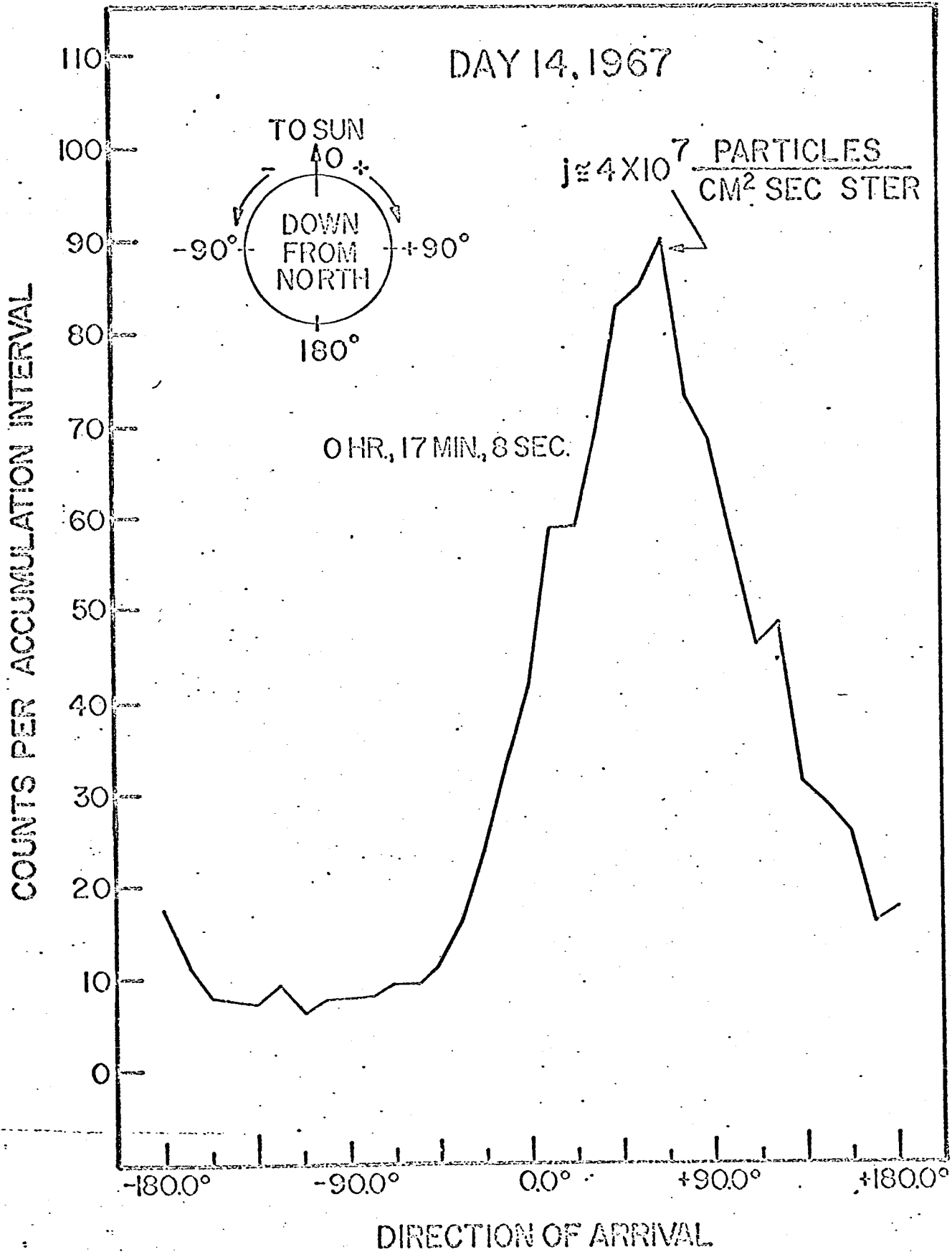
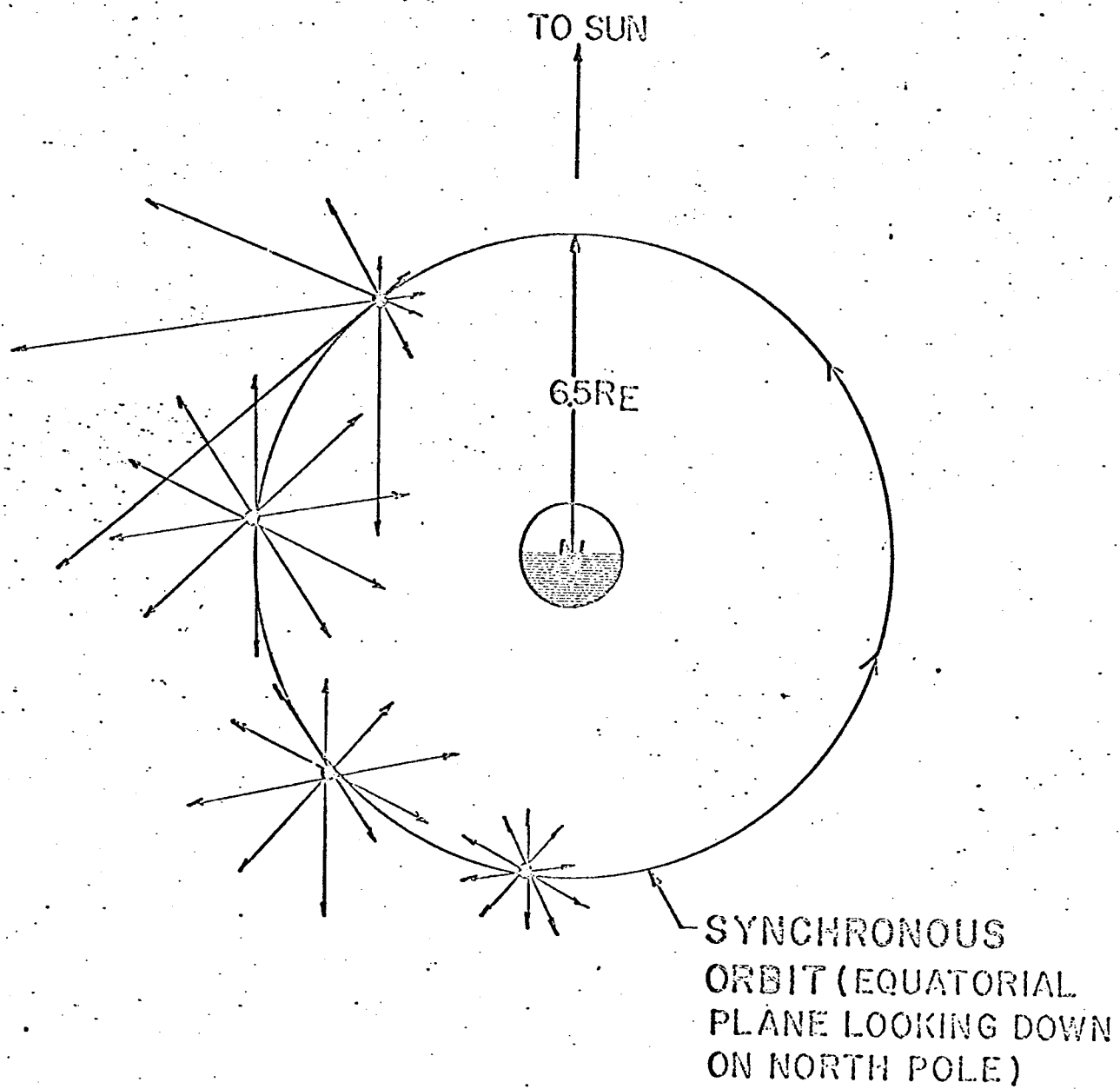


Figure 8



ANISOTROPIC PARTICLE FLUX  
DAY 14, 1967

Figure 9

THREE ISOTROPIC BURSTS  
DAY 14, 1967

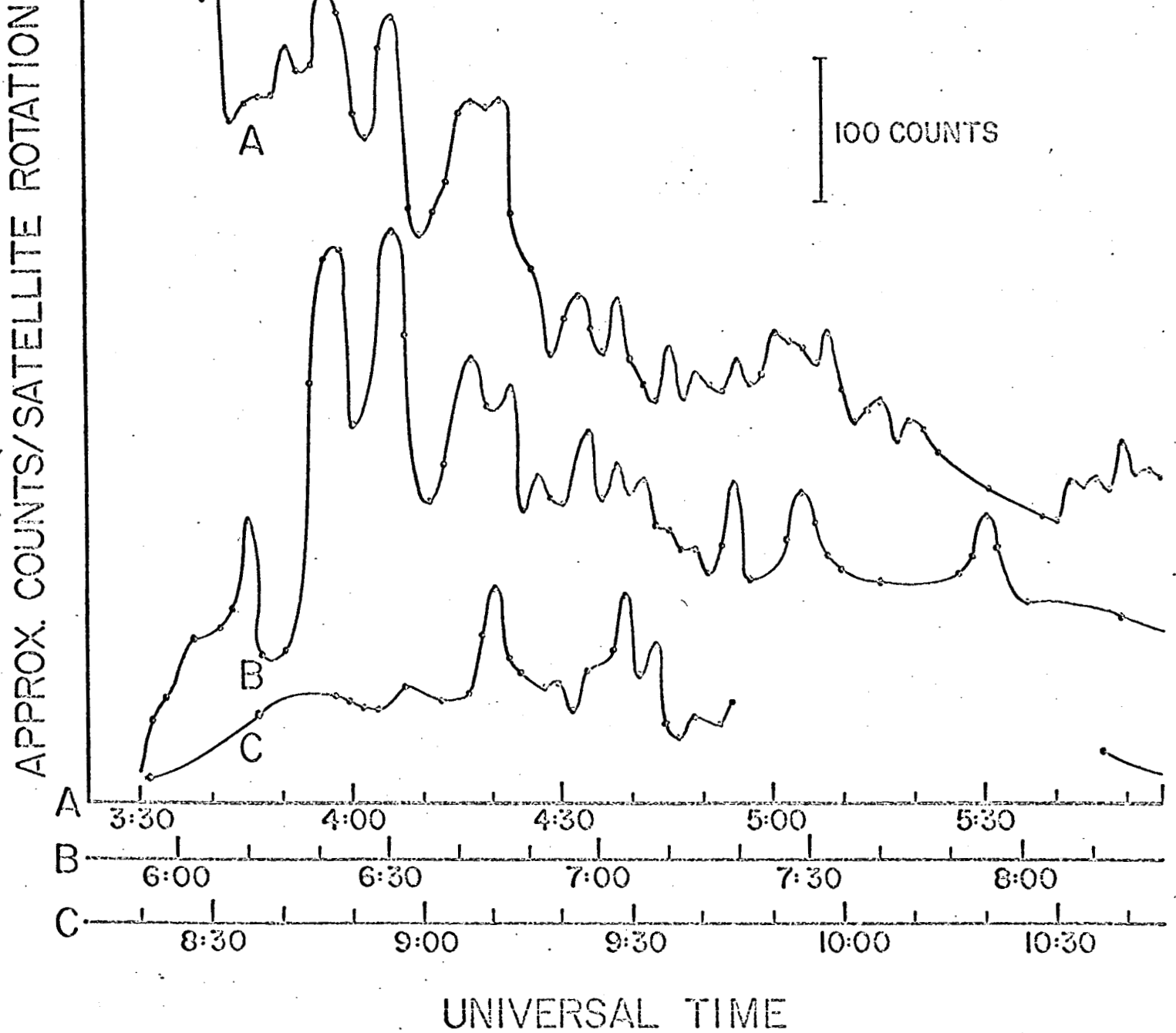


FIGURE 10

ATS-1  
 PROTONS,  $E < 50$  ev ANGULAR  
 DISTRIBUTION 8 JAN 1967  
 0146 U.T. LOOKING DOWN  
 FROM NORTH

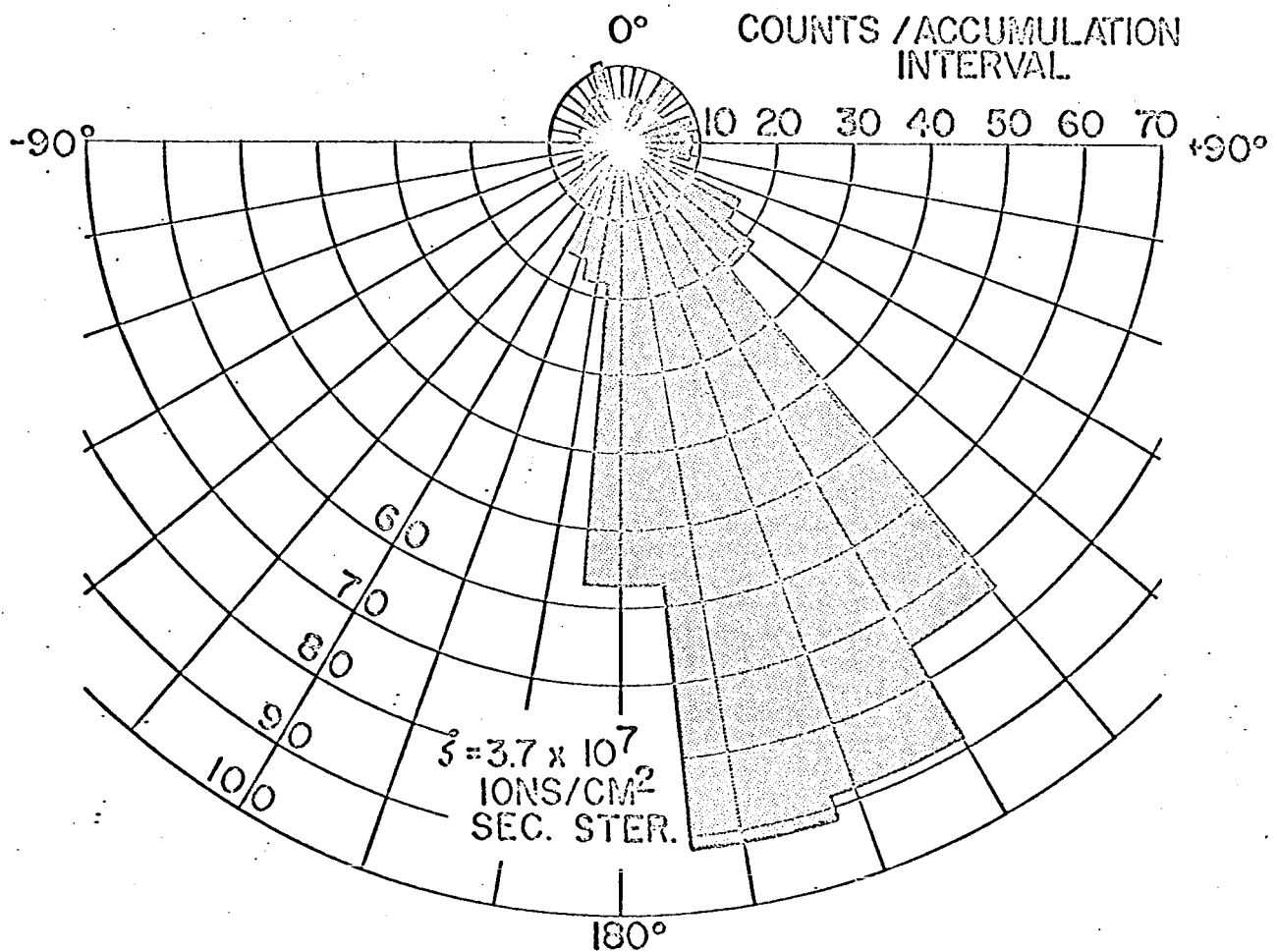
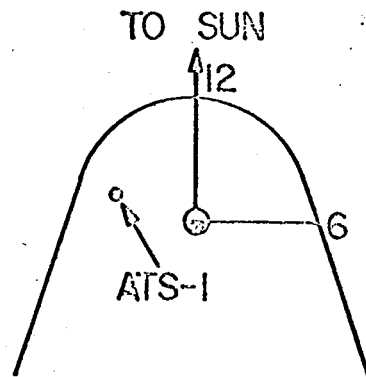
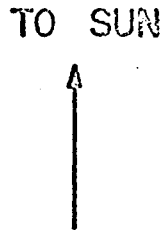


Figure 11